

2025, vol. 94, 126–138

https://doi.org/10.12657/denbio.094.009

Yuanfa Li*, Liting Wei

Spatial patterns at the structural type level of an old-growth forest in South China

Received: 30 July 2025; Accepted: 27 September 2025

Abstract: Spatial structure plays a vital role in forest operation, community dynamics, biodiversity conservation, and ecological functions, and it has been well documented at population, community, and regional levels. However, most studies on spatial structure focus on tree attributes without considering the relationships among neighbors. Based on the position, species, and size of neighboring trees, forest spatial structure can be classified into distribution, mixture, and differentiation classes. We analyzed the spatial patterns of these types in a 6-ha old-growth forest plot in southern China using pair correlation functions, mark correlation functions, and mark variogram functions. The results revealed that: (1) The distribution classes primarily exhibited aggregated patterns, with random associations dominating their relationships; (2) The mingling classes also exhibited aggregation, with spatial associations shifting from attraction to repulsion as the mingling degree increased; (3) The spatial structure of the differentiation classes was predominantly characterized by aggregation and random association. Intraspecific aggregation and small-tree aggregation were common features across all structural types. These findings are well explained by forest ecology theories such as dispersal limitation, mingling-size hypothesis, and the Janzen-Connell hypothesis, suggesting that different tree groups play distinct roles in forest communities. This study enhances our understanding of spatial structure in natural forest ecosystems and contributes to the monitoring, assessment, and management of forest resources.

Keywords: distribution pattern, nearest neighbors, size differentiation, species mixture, structural type

Addresses: Y. Li, L. Wei, Key Laboratory of National Forestry and Grassland Administration on Cultivation of Fast-Growing Timber in Central South China, Guangxi Key Laboratory of Forest Ecology and Conservation, College of Forestry, Guangxi University, Nanning 530004, China Y. Li, Laibin Jinxiu Dayaoshan Forest Ecosystem Observation and Research Station of Guangxi. No. 95 Gongde Road, Jinxiu County, Laibin, Guangxi, China 545700; https://orcid.org/0000-0001-9677-0752, e-mail: 43294659@qq.com

* corresponding author

Introduction

Forests are three-dimensional physical organisms (Spies, 1998) with broad-ranging structures and multiple forms related to their species, individual size, abundance, and shape, as well as their configuration in time and space (Hui et al., 2019; Dorji et al., 2021; Remadevi et al., 2023). In terms of space, forest

structure can be divided into vertical and horizontal components (Bohlman, 2015; Hui et al., 2019). And more and more studies from forest ecosystems emphasize the importance of spatial structure (McIntire & Fajardo, 2009; Hui et al., 2019; Li et al., 2022), as it is closely related to environmental conditions, resource availability (Martens et al., 2000; Lv et al., 2023), biodiversity, productivity (Zhang et al., 2021),

community stability, stress resistance, and resiliency (Schneider et al., 2019; Zhang et al., 2021), reflecting the trend of community succession. Spatial structure is also the result of tree growth and its integrated response to exogenous disturbances, such as drought. Thus, the spatial structure of a forest significantly affects forest management decision-making, guidelines, technology applications, and the evaluation of policy outcomes (Carrer et al., 2018).

A remarkable feature of spatial structure is the scale effect, the properties of which change continuously depending on the observation scale. A large scale reflects the influence of habitat heterogeneity on the tree point pattern, dynamics and demographics of forest communities (Getzin et al., 2008; Shen et al., 2013), while a small scale is the main domain of tree interactions (Potvin & Dutilleul, 2009; Erfanifard et al., 2018), including between individual trees and the environment, and often determines structural features that differ markedly from those observed at other scales, including species diversity, abundance, and microhabitat (Pinzon et al., 2018; Zhang et al., 2021). Small-scale spatial structure and dynamics have become an important basis for understanding forest ecological processes such as regeneration, growth, competition, dependence, death, and decomposition, as well as predicting the formation and maintenance mechanism of species diversity (Getzin et al., 2006). However, regardless of scale, most studies focus on spatial structures related to tree attributes, especially appearance characteristics, such as life stage, tree size, growth status, life form, species composition, and forest community type (Carrer et al., 2018; Engone Obiang et al., 2019; Bianchi et al., 2021). The failure to consider relationships among trees has resulted in an inadequate understanding of forest spatial structure (Zhang et al., 2021).

According to our knowledge, the relationship of nearest neighbors can provide a new approach to the analysis of forest spatial structures. A forest can be considered as a collection composed of n structural units (Zhang et al., 2018; Zhang & Hui, 2021; Li et al., 2022). In a structural unit of four trees, species distribution pattern, species mixing and size differentiation of adjacent trees *j* surrounding reference tree i are well described by a group of indices, including the uniform angle index (W), species mingling (M) and dominance (U) (Fig. A1). These parameters are independent of each other (Li et al., 2022; Remadevi et al., 2023), with the uniform expression and the exact same value hierarchy 0, 0.25, 0.50, 0.75, and 1.0 (Kint et al., 2003; Zhang et al., 2019). Each value class has a clear biological significance and is easily recognizable in woodlands (Hui et al., 2019). Based on these characteristics, forest stands can be divided according to the distributions, mixing and size differentiation of their tree groups, which define what "structural types" in this study. Among them, distribution classes are composed of highly regular trees (HRT), regular trees (ReT), random trees (RaT), clumped trees (CT), and highly clumped trees (HCT) (Zhang et al., 2018). Mixture classes can be divided into null mixed (NMT), low mixed (LMT), medium mixed (MMT), high mixed (HMT), and completely mixed trees (CMT), and differentiation classes comprise dominant trees (DoT), sub-dominant trees (SDT), medium-sized trees (MST), weak trees (WT), and absolutely weak trees (AWT) (Li et al., 2020). The structural types are tree communities that are lower than the stand but higher than the single tree level (Table 1). To date, the properties of these structural types remain unknown.

The distribution pattern, spatial associations, and tree marks are the three most important aspects of forest spatial structure (Condit et al., 2000; McIntire & Fajardo, 2009; Birch et al., 2019). Since the objects included in the distribution class, the mixture class, and the differentiation class are different, we

Table 1 Structure	tymac bacac	on the creatial	rolationchine of	f nearest neighbors
Table 1. Suluctula	l types basec	i on the spatial	Telationsinps of	l licarest licigilibors

Formulas	Patterns	Values	Structural types		References
1 50	$4 \alpha_j \ge \alpha_0$	$W_i = 0.00$	highly regular tree	HRT	(Hui et al., 2019)
$W_i=rac{1}{4}\sum_{j=1}^4 Z_{ij}$,	$3 \alpha_j \ge \alpha_0$	$W_i = 0.25$	regular tree	ReT	
$Z_{ij} = \begin{cases} 1, & \text{if } \alpha_j < \alpha_0 = 72^{\circ} \\ 0, & \text{otherwise} \end{cases}$	$2 \alpha_j \geq \alpha_0$	$W_i = 0.50$	random tree	RaT	
	$1 \alpha_j \geq \alpha_0$	$W_i = 0.75$	clumped tree	CT	
	$0 \ \alpha_j \geq \alpha_0$	$W_i = 1.00$	highly clumped tree	HCT	
1	$4 sp_i \neq sp_i$	$M_i = 0.00$	non-mixed tree	NMT	(Hui et al., 2019)
$M_i = rac{1}{4} \sum_{j=1}^4 V_{ij}$,	$3 sp_i \neq sp_i$	$M_i = 0.25$	low mixed tree	LMT	
(1:6/	$2 sp_j \neq sp_i$	$M_i = 0.50$	medium mixed tree	MMT	
$V_{ij} = \begin{cases} 1, & \text{if } sp_j \neq sp_i \\ 0, & \text{otherwise} \end{cases}$	$1 sp_i \neq sp_i$	$M_i = 0.75$	highly mixed tree	HMT	
(o, otherwise	$0 sp_j \neq sp_i$	$M_{i} = 1.00$	completely mixed tree	CMT	
1	$4 d_j < d_i$ $3 d_j < d_i$	$U_i = 0.00$	dominant tree	DoT	(Hui et al., 2019)
$U_i = \frac{1}{4} \sum_{j=1}^4 K_{ij}$,	$3 d_i < d_i$	$U_i = 0.25$	sub-dominant tree	SDT	
(\circ) if $d < d$	$2 d_i < d_i$	$U_i = 0.50$	medium sized tree	MST	
$K_{ij} = \begin{cases} 0, & \text{if } d_j < d_i \\ 1, & \text{otherwise} \end{cases}$	$1 d_j < d_i$	$U_{i} = 0.75$	weak tree	WT	
(1, otherwise	$0 d_j < d_i$	$U_i = 1.00$	absolutely week tree	AWT	

hypothesized that their spatial patterns vary greatly, and dataset from an old-growth forest in southwestern China were used to reveal the spatial patterns of structural types and the results was explained. This approach is conducive to understanding the nature of forest communities. The results of this study will have multiple implications for forest resource monitoring and quality improvement, ecosystem services and functions, and biodiversity conservation.

Materials and methods

Study sites

Our field study was conducted at Guangxi Dayaoshan National Nature Reserve, located in Jinxiu Yao Autonomous County, Laibin City, Guangxi Zhuang Autonomous Region (109°50'–110°27'E, 23°40'–24°28'N), China. The total area of the study site is 25594.7 ha, with an elevation of 513–1321 m, annual sunshine duration of 1268.7 h, average annual temperature of 17 °C, and annual precipitation

of 1823.9 mm. The study area, which is a rainfall center of Guangxi, is surrounded by seven counties: Mengshan, Lipu, Luzhai, Xiangzhou, Wuxuan, Guiping and Pingnan. The complex terrain of the region includes the Shengtang Group peaks, lower-altitude mountains, high and low hills, and various Danxia landforms. Within the reserve, wildlife populations such as Cathaya argyrophylla Chun & Kuang, Bretschneidera sinensis Hemsl., Taxus wallichiana var. mairei (Lemee & H. Léveillé) L. K. Fu & Nan Li, Sauvagesia rhodoleuca (Diels) M.C.E. Amaral, Mussaenda shikokiana Makino, Euryodendron excelsum Hung T. Chang and Dayaoshania cotinifolia W. T. Wang are protected as are evergreen broadleaf forest ecosystems. The reserve lies within the transitional region between the south and middle tropics, and its vegetation is composed of 27 phytoformations: 9 evergreen broadleaf forests, 11 monsoon evergreen broadleaf forests, 2 seasonal rainforests, 3 mid-mountain coniferous broadleaf mixed forests, and 2 hilltop moss formations. In 2013, there were 947 species in 445 genera and 157 families, including 107 dicotyledonous plants and 16 gymnosperms in 7 families and 10 genera.

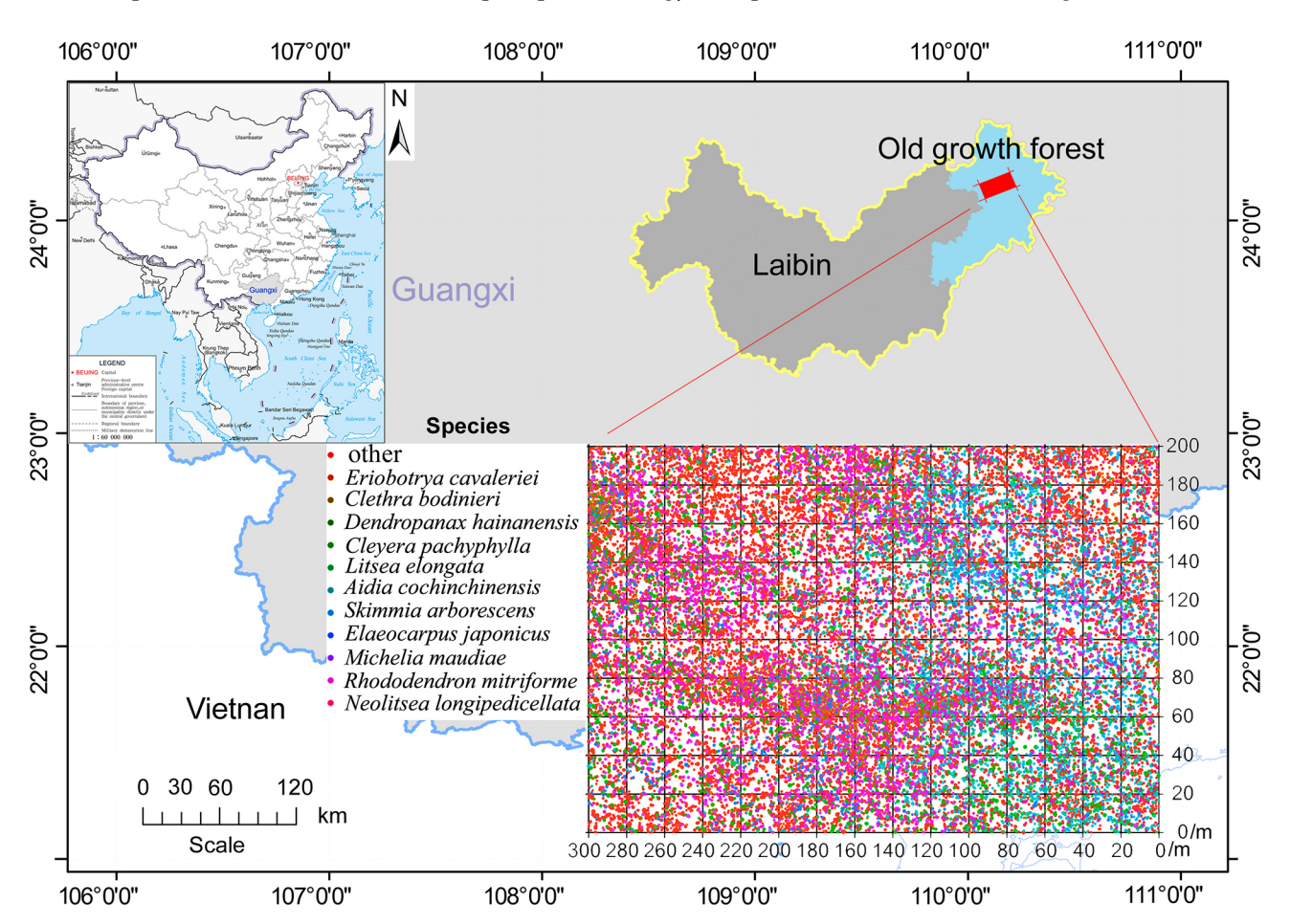


Fig. 1. Study site and tree positions. Colored dots represent populations with abundance ranked below 12th in the oldgrowth forest

Plot establishment

A standard fixed plot of 6 ha (110°14'51.06"E, 24°09'55.47"N) was established in 2018-2019 in an evergreen broadleaf forest. The plot was set up according to the criteria of the Center for Tropical Forest Science of the Smithsonian Tropical Research Institute (Condit, 1995). First, an old-growth stand was selected and a total station (NTS-372R₁₀, Southern Mapping Company, Guangzhou, China) was used to determine the four boundaries of the quadrat, and then the quadrat was divided into 150 sub-quadrats (20 m \times 20 m), which were further divided into 16 small quadrats (5 m \times 5 m), in which the position of each tree was plotted (x, y) and the tree species identified. The tree height (m), DBH (cm), height of the first branch (m), crown width (m²), and the growth state of each tree (e.g., tilt, bend, dieback, diseases, and pests) were recorded for a total of 39,733 living trees belonging to 144 species, 90 genera, and 48 families (Fig. 1).

Data analyses

Classification of structural types

First, the values of W_i , M_i , and U_i were calculated for each tree in the quadrats using an online program, see http://winkelmass.cn/intros. These three variables were then classified according to their value levels (0, 0.25, 0.50, 0.75, 1.0) and their basic quantitative information was analyzed, resulting in a total of 15 structural types (Table 2, Fig. A1). To eliminate edge effects, a buffer of 5 m was set when calculating the parameters; i.e., all trees within 5 m of the boundary of the plot were regarded as adjacent trees, whereas trees in the core area were considered both adjacent and reference trees (Li et al., 2022). The number of individuals for each type is counted only

in the core area. The distributions of trees of each structural type are shown in Fig. 2.

Distribution pattern and spatial correlation

A univariate distribution model $g_{11}(r)$ of the pair correlation function (PCF) was used to analyze the point distribution of structural types. The g₁₁(r) model calculates the number of trees within a circle with radius r centered on any tree, which well describes the change in forest distribution type with scale (Getzin et al., 2006; Getzin et al., 2008). As soil and microclimate data were not available, we applied the commonly used complete spatial randomness (CSR) model as the null model, and the maximum radius r of the circle was set to 1/4 of the small side of the quadrat (r = 200/4 m). A Monte Carlo method was used to generate the simulation envelope. The simulation time was set as nsim = 199, and the circle width as nrank = 1. We used the edge correction setting "correction = best". Goodness of fit was tested using the setting "side = two.sided", and its significance level was set at 0.01 [alpha = $2 \times 1 / (1 + 199)$] (Baddeley et al., 2015). Observed values above, within, and below the envelope represented clustered, random, and regular distributions, respectively. The bivariate distribution model $g_{12}(r)$ of the PCF was used to analyze the spatial associations among structural types. Random labeling was set as the null model, and the residual parameters were the same as those in $g_{11}(r)$. Observed values above, within, and below the simulation envelopes were defined as positive, random/ irrelevant, and negative associations, indicating attraction, no obvious relationship, and repulsion, respectively. Data analysis and graphics generation were performed using the spatstat package (Baddeley et al., 2015, 3.0-8 version) in R (R Core Team, Vienna, Austria, 4.2.0 version).

Table 2. Basic information of 15 structural types in a 6 ha old-growth forest plot in south China

			, .		•		
Structural types	Species rich- ness	Number of individuals	Number of shrubs	Number of trees	DBH ± SD (cm)	Tree height ± SD (m)	Crown area ± SD (m²)
HRT	65	191	74	117	6.85 ± 0.59	5.40 ± 3.74	1.95 ± 1.09
ReT	127	5941	2160	3781	6.58 ± 0.11	5.29 ± 3.85	1.97 ± 1.18
RaT	141	17519	6424	11095	6.45 ± 0.06	5.35 ± 3.93	1.98 ± 1.20
CT	123	5264	1871	3393	6.71 ± 0.12	5.36 ± 3.97	1.98 ± 1.20
HCT	108	1632	573	1059	6.37 ± 0.19	5.45 ± 4.05	2.02 ± 1.24
NMT	7	61	28	33	2.78 ± 0.28	5.18 ± 3.47	1.96 ± 1.16
LMT	26	331	207	124	3.33 ± 0.17	5.00 ± 3.82	1.95 ± 1.24
MMT	52	1362	745	617	3.89 ± 0.11	5.22 ± 3.82	1.95 ± 1.21
HMT	103	5826	2574	3252	5.05 ± 0.07	5.38 ± 4.00	1.99 ± 1.22
CMT	143	22967	7548	15419	7.11 ± 0.05	5.35 ± 3.92	1.98 ± 1.19
DoT	113	6041	1494	4547	16.22 ± 0.16	5.65 ± 4.24	2.08 ± 1.27
SDT	120	6087	1955	4132	7.48 ± 0.07	5.46 ± 3.95	2.02 ± 1.19
MST	127	6065	2267	3798	4.48 ± 0.04	5.30 ± 3.80	1.98 ± 1.19
WT	125	5914	2491	3423	2.86 ± 0.02	5.21 ± 3.82	1.94 ± 1.17
AWT	124	6440	2895	3545	1.79 ± 0.01	5.13 ± 3.79	1.90 ± 1.17

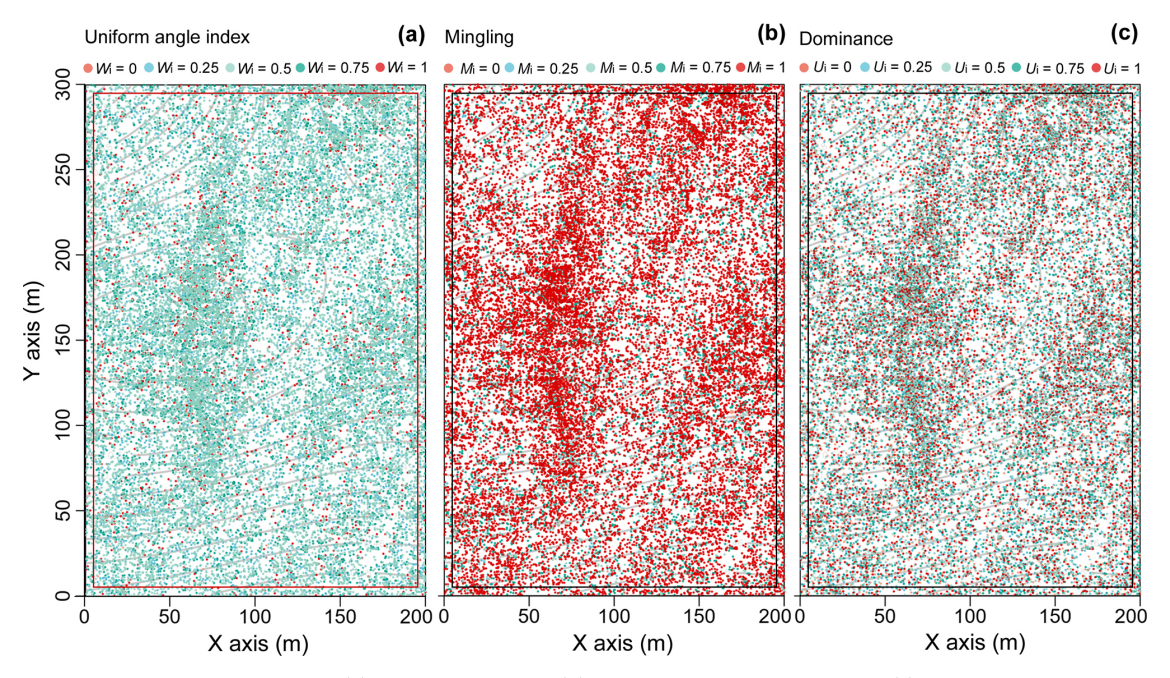


Fig. 2. Pattern of distribution classes (a), mixture classes (b), and differentiation classes (c)

Mark character

The mark correlation function (MCF) kf(r) was used to analyze the changes in tree species with observation scale. For each structural type, $k_s(r)$ measures the similarity of trees i and j at distance r. Its test function f has two parameters, $f(m_1, m_2)$, where m_1 and m_2 represent different species. The maximum observation radius r was set to 50 m, and a Monte Carlo method was used to generate a simulation envelope with 199 simulation times. We applied the edge correction setting "correction = best". Observed values above, within, and below the simulated envelope indicated conspecific aggregation/interspecific exclusion, independence, and conspecific exclusion/ interspecific aggregation, respectively (Muvengwi et al., 2018). The mark variogram function (MVF) γ (r) was used to analyze tree size similarity between the i^{th} and j^{th} trees at distance r (Getzin et al., 2010; Muvengwi et al., 2018). Tree size refers specifically to DBH, and its parameter setting was the same as that in $k_{\epsilon}(r)$. Observed values above, within, and below the simulated envelope indicated large tree clustering, size independence, and small tree clustering, respectively (Muvengwi et al., 2018). The data were analyzed using the spatstat package (Baddeley et al., 2015, 3.0-8 version) in R.

Results

Spatial patterns of distribution classes

HRT had a random distribution at r = 0–50 m (Fig. 3a); the observed values of other distribution classes were far from the upper line of the Monte

Carlo simulation envelope at most scales, and the degree of aggregation tended to increase with increasing grades of W (Fig. 3b–e). HRT was randomly associated with the other four distribution classes at each scale (Fig. 3f–i). ReT slightly repelled RaT, as well as two aggregative trees, at scales of r=4-10, 0–2, and 4–11 m, but they had a random association at the remaining scales (Fig. 3j–l). RaT and two aggregative trees were mildly attracted at some scales, but maintained random association at most scales (Fig. 3m–n). Similarly, the two aggregative trees were mutually attractive at r=0-4 and 7–28 m, but showed a random correlation at r=28-50 m (Fig. 3o).

Spatial pattern of mixture classes

With the exception of r = 27-30 m, the class NMT was distributed in clusters (Fig. 4a). LMT was randomly distributed at r = 5-10, 14-25, and 32-45 m, but was clustered at other scales, similar to MMT (Fig. 4b–c). However, the scale of aggregation of HMT expanded to r = 0-38 m, and that of CMT to every scale (Fig. 4d-e). In most cases, NMT and low to medium mixed trees were mutually attractive (Fig. 4f-g), but randomly correlated with HMT and repulsed CMT (Fig. 4h, i). LMT and MMT were mutually attractive at r = 0-6, 14–16, and 24–26 m, but were randomly correlated at other major scales (Fig. 4j). LMT repulsed HMT at r = 0-3 and 10-41 m, whereas the degree and scale of the repulsion of CMT were further expanded (Fig. 4k, 1). The spatial association between MMT and two highly mixed trees was dominated by exclusion (Fig. 4m-n), but the latter were mutually repulsive only at r = 0-4 m (Fig. 40).

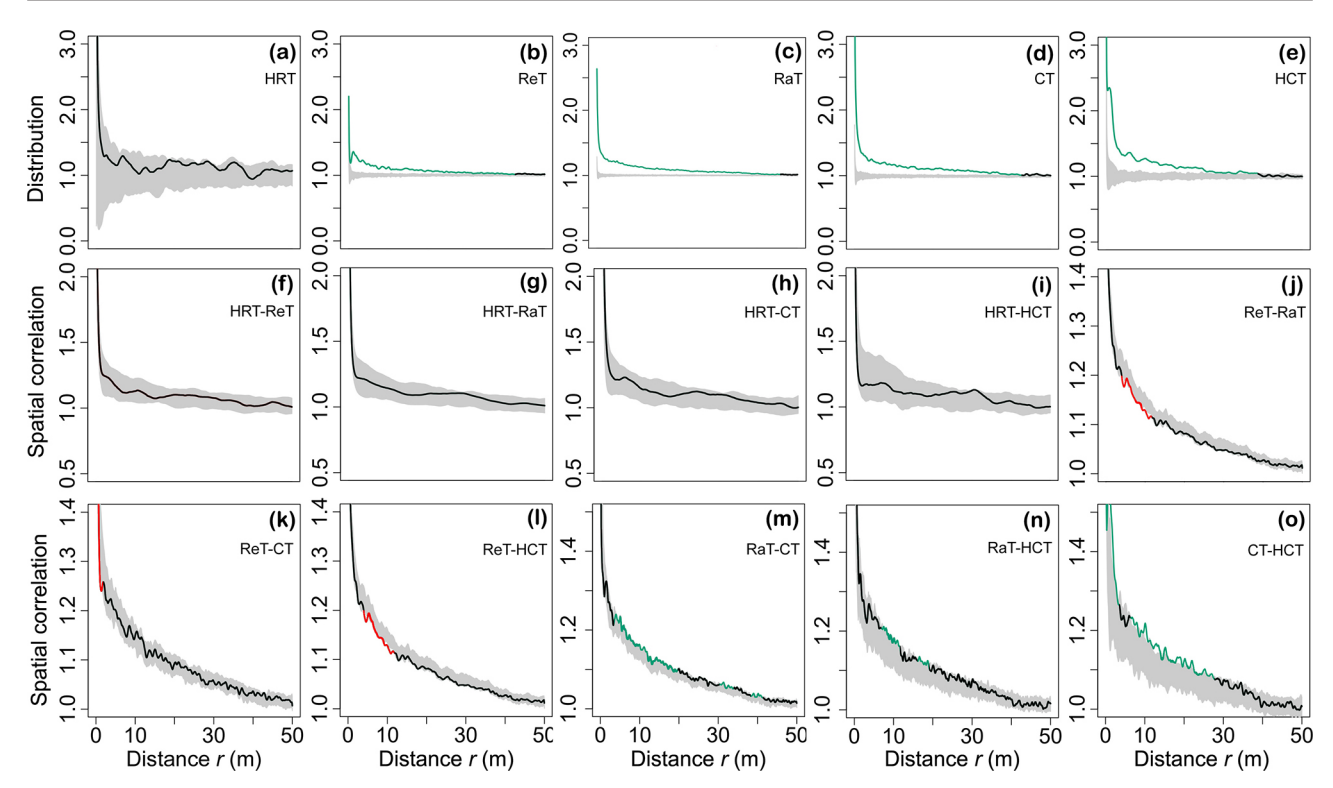


Fig. 3. Distribution patterns and spatial correlations of distribution classes. Solid lines indicate observed values, and the gray areas indicate the 95% Monte Carlo simulation envelope. Green lines indicate clusters (a–e) and attraction (f–o), red lines indicate regularity (a–e) and repulsion (f–o), and black lines indicate random pattern (a–e) and correlation (f–o). Explanations for figures are the same as following

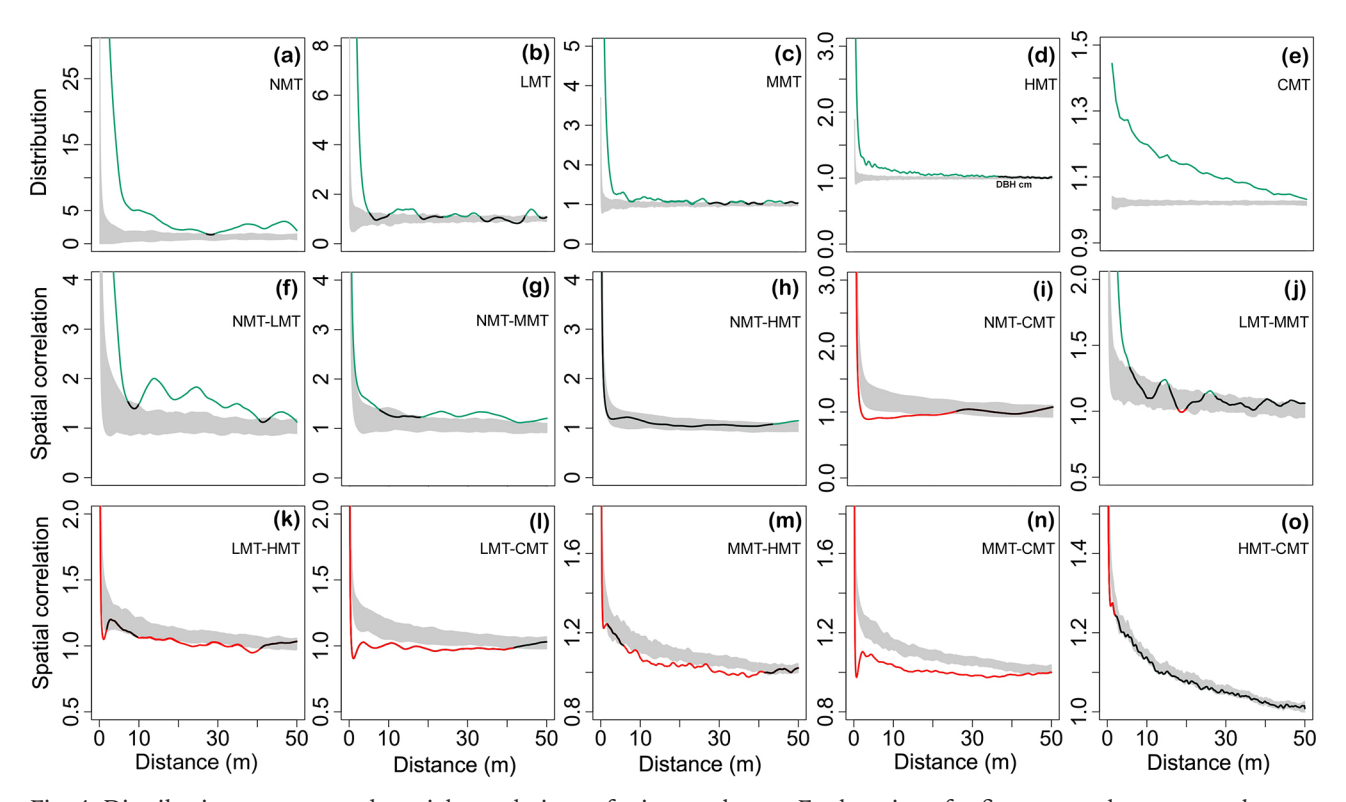


Fig. 4. Distribution patterns and spatial correlations of mixture classes. Explanations for figures are the same as above

Spatial pattern of differentiation classes

The distribution patterns of the four differentiation classes were very similar. They were regularly distributed at r = 0-1 m, maintained aggregation at a scale of approximately r = 1-45 m, and then assumed

a random distribution at larger scales (Fig. 5a–e). In addition to correlation pairs that were positively correlated at r=0-1 m, the spatial correlation between any two other differentiation classes was also very similar, with random correlations maintained at r=1-50 m (Fig. 5f–o).

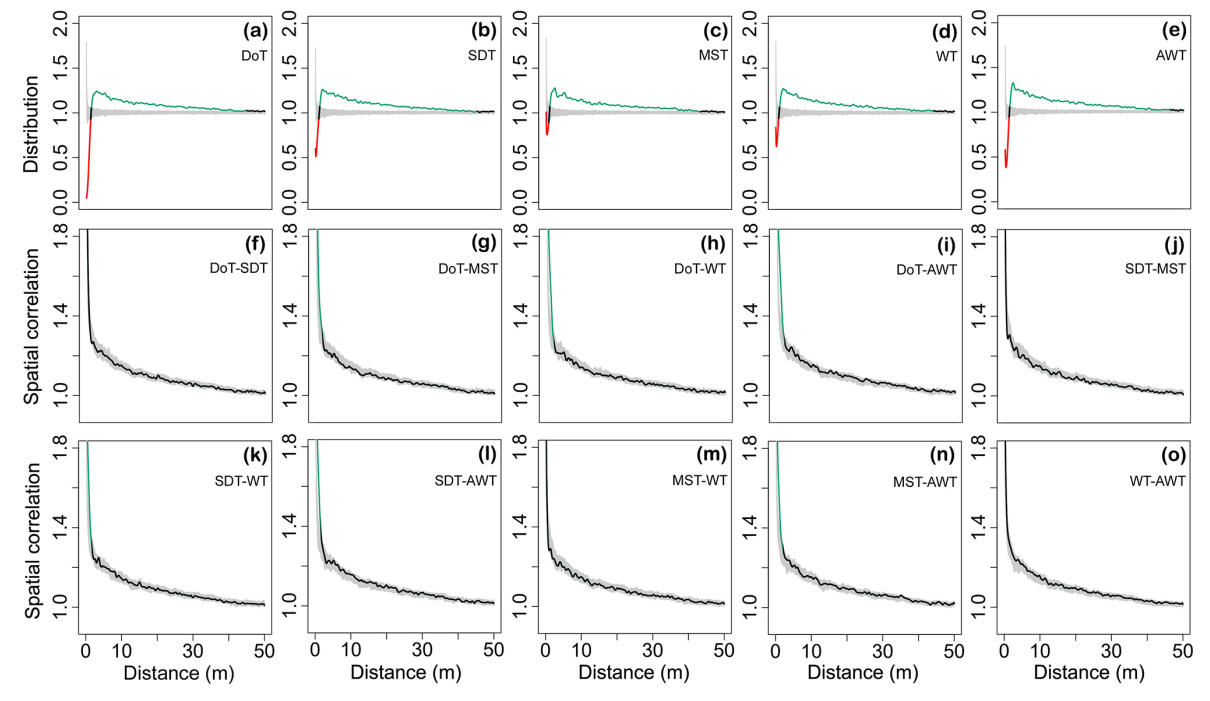


Fig. 5. Distribution patterns and spatial correlations of the differentiation classes. Explanations for figures are the same as following

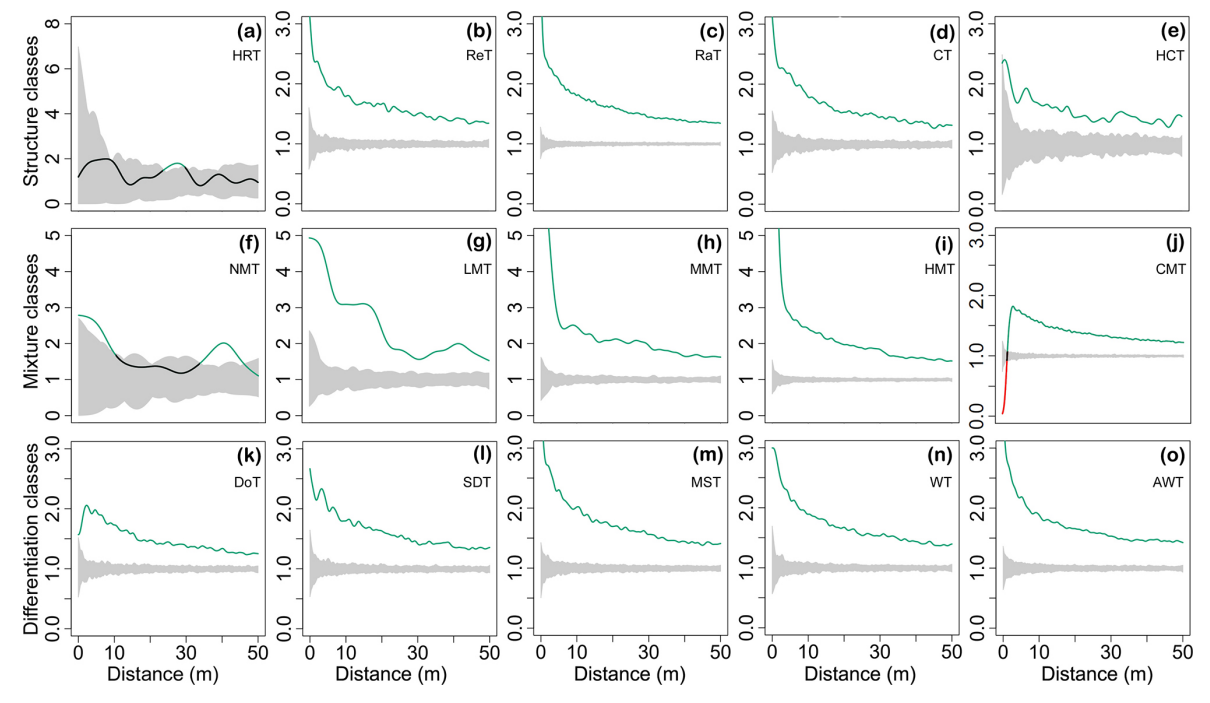


Fig. 6. Tree species spatial distribution. Solid lines indicate observed values, and gray shading indicates the 95% Monte Carlo simulation envelope. Green and red lines indicate intra- and interspecific clusters, respectively, and black lines indicate a random pattern of tree species

Mark character of structural types

The tree species of HRT showed intraspecific aggregation at r = 20–26 m, but had a random pattern at other scales (Fig. 6a). All observed values of the other four distribution classes were much higher than the upper line of the Monte Carlo simulation envelope, implying intraspecific aggregation (Fig. 6b–e). The tree species of NMT showed intraspecific aggregation at small and large scales (r = 0–1, 33–46 m), but were randomly distributed at medium scales. The intraspecific aggregations of LMT, MMT, and HMT were obvious (Fig. 6f–i). CMT showed a similar trend, with interspecific isolation at r = 0–1 m (Fig. 6j). Clear intraspecific aggregation of differentiation classes was also observed, and the intensity decreased as the scale increased (Fig. 6k–o).

The tree sizes included in HRT and HCT were randomly distributed (Fig. 7a, e). For ReT, small trees were clustered at r = 3–40 m, whereas trees of different sizes were randomly distributed at other scales (Fig. 7b). RaT and CT had a similar tree size distribution, with small trees clustered at r = 0–42 m and trees of different sizes randomly distributed at larger scales (Fig. 7c, d). The tree sizes of NMT were randomly distributed (Fig. 7f), whereas small trees of LMT and MMT clustered within various scales and residual trees were randomly distributed in others (Fig. 7g, h). Small trees of HMT and CMT aggregated at scales r = 0–31 and 0–50 m (Fig. 7i, j). The tree sizes within the different differentiation classes

showed a similar pattern; that is, except for random distribution of a small portion of trees at the large scale, residual observed values were below the Monte Carlo envelope (Fig. 7k–o).

Discussion

Structural properties of distribution classes in natural forests

Distribution patterns indirectly reflect the successional process of forest communities (Getzin et al., 2008). Aggregation occurs widely in natural forests, especially within stands in the early succession stages (Wang et al., 2018; Bastias et al., 2019; Engone Obiang et al., 2019; Lv et al., 2023). The much lower abundance of HRT than of HCT indicated aggregation distribution within the old-growth forest on the Dayao Mountain (Zhang & Hui, 2021). The relationship between HRT and its nearest neighbors was absolutely uniform, and spaces among individuals were large in some cases, which is often understood as the result of intense competition (Engone Obiang et al., 2019). This finding may also be the main explanation for the random distribution and random association of this structural type with residual distribution classes. Tree population sizes also affect the types of distribution pattern (Zhao et al., 2014). Residuals support the aggregation of communities, which can be caused by many biological or abiotic

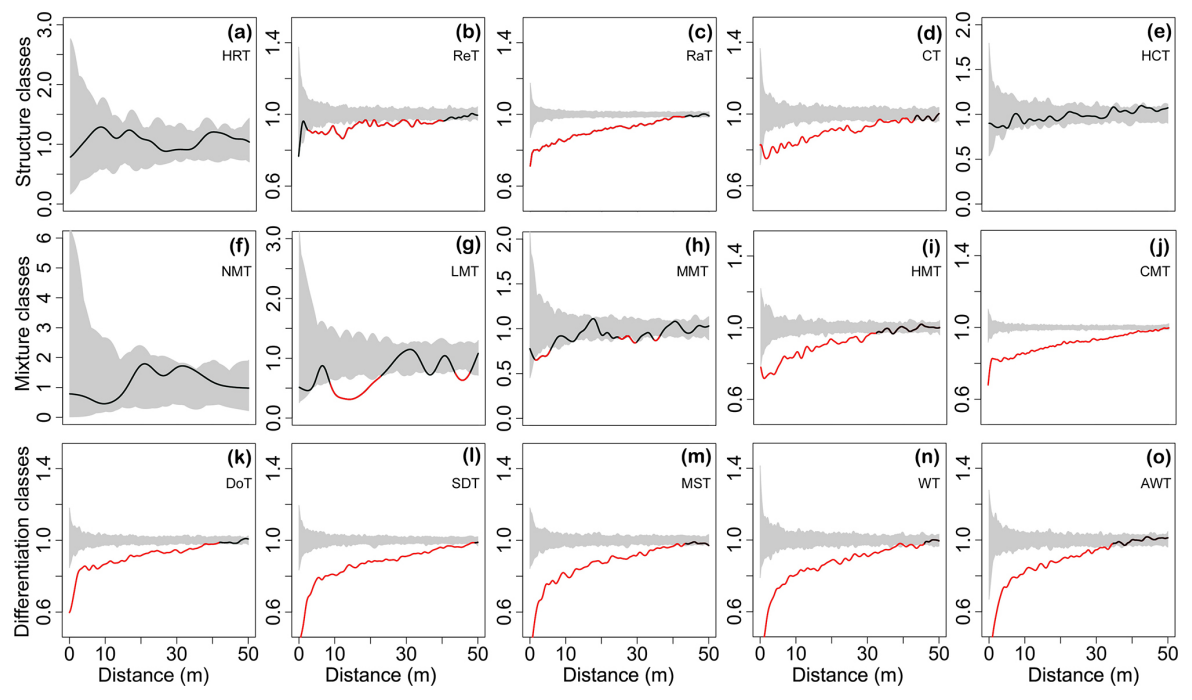


Fig. 7. Tree size spatial distribution. Solid lines indicate observed values; gray shading indicates the 95% Monte Carlo simulation envelope. Red and black lines indicate clusters of small trees and random tree size, respectively

factors (Bastias et al., 2019; Li et al., 2022). In the studied forest, CT and HCT maintained their aggregative characteristics within the structural unit and were mutually attractive, which would likely result in the formation of larger clumps. Regular and random trees were also clustered, suggesting that classification revealed the clustering intensity of the distribution pattern. The distribution pattern of distribution classes also showed that the results of the nearest neighbor analysis (W) and spatial function g(r) are not always consistent, with the latter producing more clustering (Ghalandarayeshi et al., 2017). Nearest neighbor analysis is instructive with respect to expression, sampling, and practice (Bettinger & Tang, 2015; Hui et al., 2019; Zhang et al., 2019), whereas spatial functions provide more reliable information on outcomes and ecological processes (Kint et al., 2003; Ghalandarayeshi et al., 2017), although they are heavily influenced by the null model (Carrer et al., 2018). Targeted selection or the simultaneous use of both a nearest neighbor analysis (W) and a spatial function g(r) may be more conducive to fully revealing the characteristics of stand structures.

The species included in HRT were randomly distributed, and their abundance accounted for approximately half of the total community. Higher richness of other distribution classes was associated with stronger species aggregation. As most populations in natural forests are clustered (Wang et al., 2018; Engone Obiang et al., 2019), the probability that the nearest neighbor of a species, especially a rare species, is a tree of the same species will be higher than the community average of the occurrence of that species (Condit et al., 2000; Nguyen et al., 2016), supporting our results. However, in other distribution patterns, the distribution of richness among structural types and its effect on tree species distribution are unclear, given the small number of natural forests with a regular or random distribution and the paucity of studies of those forests (Li et al., 2022). Tree size distribution is also related to structural types. Differences in DBH may determine the spatial distribution of tree size, where smaller differences indicate greater probability of a random distribution, and vice versa. The tree sizes of HCT and HRT were randomly distributed, and the maximum and minimum diameters of those trees were average. RaTs accounted for approximately 50% of the trees of each diameter size class in natural forests (Zhang & Hui, 2021; Li et al., 2022), but the extremes in DBH included many small trees that formed a clump. In natural forests with distinct vertical stratifications, including the study forest, the upper layer has an obvious aggregation pattern of tree size that is significantly different at DBH, whereas tree size in the the lower layer is likely have a more random pattern (Ghalandarayeshi et al., 2017; Pommerening et al., 2020). The relationship between tree size and distribution pattern is mainly responsible for the particular resource utilization strategy. Gap regenaeration and seed dispersal limitation result in sapling aggregation, with their competition leading to size differentiation, high mortality, and increasing neighbor distance.

Structural properties of mixture classes in natural forests

Aggregation is a common characteristic of mixture classes. Both the mixing pattern and the distribution pattern affect neighbor interactions (Potvin & Dutilleul, 2009), regulate tree growth processes, and may increase tree mortality (Bastias et al., 2019). Conversely, the death and regeneration of natural forests simultaneously alter the distribution pattern and mixing status, consistent with the absence of an absolute relationship between distribution pattern and mingling. In natural pure and mixed European beech forests, proximate trees are randomly distributed (Petritan et al., 2012). Thus, the species composition and diversity of natural forests in different climatic regions of China may differ; however, the distribution eventually becomes random (Zhang et al., 2018). Our results are strongly supported by previous findings that the degree of mixture in multispecies forests is independent of the distribution pattern (Xu et al., 2006; Li et al., 2020). However, using a computer simulation, Wang et al. (2016) found that a random distribution has no effect on the species mixture, whereas it is reduced by aggregation and increased by regular distribution. Nonetheless, if biological interactions are not considered, simulations do not always provide realistic scenarios. In mixed forests, the distribution pattern of a tree species is always related to that of other tree species (Graz, 2004), with both a high level of mixture and aggregative distribution common at the community level.

Individuals of the two low-mixing classes were small and mutually attractive, suggesting conspecific aggregation that was likely caused by gravitational seed and dispersal limitation (Ghalandarayeshi et al., 2017; Wang et al., 2018; Engone Obiang et al., 2019). However, habitat preference, habitat filtering, disturbance and reproductive behavior can also enhance the aggregation of populations (Getzin et al., 2008; Shen et al., 2013; Bastias et al., 2019). Particularly in alpine regions, complex terrain plays a secondary role in the distribution of habitat resources (Lv et al., 2023), altering species distribution and interspecific associations, and strengthening species-habitat associations (Shen et al., 2013). As the mixture grade increased, the spatial association of mixture classes changed from attraction to randomness, and then to repulsion, such that greater differences in the

mixture grade were associated with more obvious repulsion. These observations indicate that the species composition of a community forms a mosaic of pure forest and mixed forest in space, potentially leading to a decrease in species aggregation with an increase in scale that influences future community development (Carrer et al., 2018). A mosaic distribution is a typical attribute of aged forests (Spies, 1998; Getzin et al., 2008), as it is directly related to species interaction and resource utilization (Shen et al., 2013), but also reflects internal and external ecological processes. Homospecific attraction and heterospecific repulsion reflect the simultaneous occurrence of multiple ecological processes in the aged forest (Carrer et al., 2018). In species-rich tropical forests, high species diversity leads to lower density, which in turn leads to complex intra- and interspecific interactions (Nguyen et al., 2016).

The quantitative distribution of individuals within the mixture classes of the old-growth forest on Dayao Mountain was similar to that in many other natural forests (Li et al., 2020; Lv et al., 2023); that is, only a small proportion of small trees were the same species as their closest neighbors. The sizes of these small trees were randomly distributed in space, suggesting that the probability of conspecific negative density dependence was either low or not obvious, in contrast to the mechanism of species diversity maintenance in tropical and other subtropical natural forests (Paine et al., 2012; Comita et al., 2014; Zhu et al., 2015). Due to multiple factors (Birch et al., 2019), conspecific negative density dependence may be weak in montane climax communities. Larger individuals have higher degrees of mingling, which is consistent with the conclusion that diameter is linearly related to the mixing degree (Li et al., 2020) and supports the mingling-size hypothesis (Wang et al., 2018; Pommerening et al., 2020). Most large interspecifics in the studied forest were uncommon species that provided shelter for small trees (Zhu et al., 2015), as proposed by the Janzen– Connell hypothesis (Comita et al., 2014; Nguyen et al., 2016). AWT implies heterospecific aggregation within at least a structural unit, and its higher values indicate that heterospecific aggregation is prevalent in this community, accounting for the high degree of mixture in the community at a very small scale. Bastias et al. (2019) suggested that trees in communities with higher richness and functional diversity are closer to each other, which supports our results and is consistent with the status of Dayao Mountain as a global biodiversity hotspot (Li et al., 2023). Despite the importance of studying the mechanism of species coexistence by combining heterospecific effects, this approach is often neglected (Wang et al., 2018). In our consideration of the effect of scale, intraspecific aggregation dominated the species distribution of the community, indicating that species mixture is related to scale. Additionally, the increase in mingling and enhanced aggregation of small trees were synchronized, suggesting that heterospecific small trees promote a high degree of mixing within the community. Rare species are important components of species diversity in aged forests (Li et al., 2023); they are typically smaller and exhibit higher aggregation than common species (Condit et al., 2000). In addition to tree death, the emergence of rare species is an important driver of mixture pattern changes.

Structural properties of differentiation classes in natural forests

Among differentiation classes, both DoT and SDT contained many small trees with smaller proportions than in inferior classes (WT and AWT). This finding suggests that some structural units in the plot were dominated by small trees; however, more often, small trees coexisted with large trees, as also observed by Pommerening et al. (2020). The coexistence of small and large trees may favor reduced competition and the maintenance of community stability, as shown by the random association of various differentiation classes. Although differentiation classes in the study area had a similar clumped distribution pattern, many other studies have found that both the upper layer of large trees and large trees in old stands tend to have a regular or random distribution, whereas small trees, understory trees, and young stands tend to have a clustered distribution (Condit et al., 2000; Getzin et al., 2006; Wehenkel et al., 2015; Wang et al., 2018; Zhang et al., 2018), there are also counterexamples (Li et al., 2008). Dominant trees at the structural type and stand levels belong to different categories (Li et al., 2022). The former contains many small trees that enhance the aggregation intensity of the distribution pattern, whereas the latter consists of large trees that compose the community framework, completely occupy the canopy advantage, and drive community development (Engone Obiang et al., 2019; Caron et al., 2021). Thus, the relationship between size differentiation and DBH at the stand level is well expressed by a negative exponential function rather than a linear model (Li et al., 2020), thereby explaining the differences in their distribution patterns.

Recent studies have shown that the U of natural forests plays a role in 'equalization', resulting in a similar number of trees in differentiation classes (Zhang et al., 2019; Li et al., 2020; Lv et al., 2023), consistent with our results. Size differentiation always occurs within a structural unit, with reference tree *i* having a similar probability of belonging to one of these differentiation classes (Petritan et al., 2012). This possibility is further supported by the similar

tree size distribution of the differentiation classes in the study forest. Hui et al. (2019) argued that this is the most common situation in natural forests, which suggests that the spatial distribution of tree size is in a state of equilibrium rather than a neutral state. Other studies have shown that stable differentiation is an early event that occurs even in artificial forests after their near-natural conversion (Li et al., 2020), and seems to be only partially influenced by environmental factors (Lv et al., 2023). Uniform differentiation should be emphasized in forest management to maintain community structural balance. Similar species abundances and aggregation are common characteristics of differentiation classes. The slightly lower degree of species aggregation in DoT than in the other differentiation classes suggests multispecies co-dominance in this community, which is consistent with the characteristics of other natural forests near the Tropic of Cancer (Li et al., 2008; Nguyen et al., 2016; Li et al., 2023). Most research has been focused on the distribution characteristics of differentiation classes rather than their underlying mechanism. A stable quantitative distribution of differentiation classes may be more useful in competitive analysis and selection systems (Hui et al., 2018).

Conclusion

The spatial structure of forests is highly complex and can be analyzed from multiple perspectives. In this study, we classified the old-growth forest in the Dayaoshan Mountains of Guangxi, China, into 15 structural types based on nearest-neighbor relationships, and analyzed their distribution patterns, spatial associations, and mark character. These structural types exhibit various patterns, all of which can be well explained by prevailing ecological theories, thus supporting the rationale of our classification system. Each structural type plays a different role within the community, enriching our understanding of natural forest ecosystems, particularly the construction of their spatial structures, and potentially providing insights into ecological processes that are difficult to observe directly. In studies aimed at forest biodiversity conservation and monitoring, spatial structural differences should be examined at the community and structural type levels through systematic analyses at different scales, especially the fine scale; however, this approach has been largely neglected. This study also contributes to closing the knowledge gap regarding the medium-scale spatial structure of subtropical natural forests. Comparisons of forest structural types at the global or regional level and exploration of the non-spatial structure of structural types remain areas of future research.

Declarations

Ethics approval and consent to participate: Not applicable

Consent for publication: Not applicable

Availability of data and materials: The datasets used and/or analysed during the current study are available from the corresponding author on reasonable request.

Competing interests: Authors have no conflicts of interest

Funding: This work was supported the National Natural Science Foundation of China (Grant No. 32060340) and Scientific Research Capacity Building Project for Laibin Jinxiu Dayaoshan Forest Ecosystem Observation and Research Station of Guangxi (Grant No. 22-035-130-01).

Authors' contributions: Yuanfa Li conceived the idea, Yuanfa Li and Liting Wei wrote and reviewed the manuscript.

Acknowledgements

Employees from Guangxi Forest Resources and Environment Monitoring Center helped us to collect data.

References

Baddeley A, Rubak E & Turner R (2015) Spatial point patterns: methodology and applications with R. CRC Press, Chapman and Hall, London. doi:10.1201/b19708.

Bastias CC, Truchado DA, Valladares F, Benavides R, Bouriaud O, Bruelheide H, Coppi A, Finér L, Gimeno TE, Jaroszewicz B, Scherer-Lorenzen M, Selvi F & De la Cruz M (2019) Species richness influences the spatial distribution of trees in European forests. Oikos 129: 380–390. doi:10.1111/oik.06776.

Bettinger P & Tang M (2015) Tree-level harvest optimization for Structure-Based Forest Management based on the species mingling index. Forests 6: 1121–1144. doi:10.3390/f6041121.

Bianchi E, Bugmann H, Hobi ML & Bigler C (2021) Spatial patterns of living and dead small trees in subalpine Norway spruce forest reserves in Switzerland. Forest Ecology and Management 494: 119315. doi:10.1016/j.foreco.2021.119315.

Birch JD, Lutz JA, Simard SW, Pelletier R, LaRoi GH & Karst J (2019) Density-dependent processes fluctuate over 50 years in an ecotone forest. Oecologia 191: 909–918.

Bohlman SA (2015) Species diversity of canopy versus understory trees in a neotropical forest: Implications for forest structure, function and mon-

- itoring. Ecosystems 18: 658–670. doi:10.1007/s10021-015-9854-0.
- Caron TMF, Chuma V, Sandi AA & Norris D (2021) Big trees drive forest structure patterns across a lowland Amazon regrowth gradient. Scientific Reports 11: 3380. doi:10.1038/s41598-021-83030-5.
- Carrer M, Castagneri D, Popa I, Pividori M & Lingua E (2018) Tree spatial patterns and stand attributes in temperate forests: The importance of plot size, sampling design, and null model. Forest Ecology and Management 407: 125–134. doi:10.1016/j. foreco.2017.10.041.
- Comita LS, Queenborough SA, Murphy SJ, Eck JL, Xu K, Krishnadas M, Beckman N, Zhu Y & Gomez-Aparicio L (2014) Testing predictions of the Janzen-Connell hypothesis: a meta-analysis of experimental evidence for distance-and density-dependent seed and seedling survival. Journal of Ecology 102: 845–856. doi:10.1111/1365-2745.12232.
- Condit R (1995) Research in large, long-term tropical forest plots. Trends in Ecology & Evolution 10: 18–22. doi:10.1016/S0169-5347(00)88955-7.
- Condit R, Ashton P, Baker P, Bunyavejchewin S, Gunatilleke S, Gunatilleke N, Hubbell S, Foster R, Itoh A, LaFrankie J, Lee H, Losos E, Manokaran N, Sukumar R & Yamakura T (2000) Spatial patterns in the distribution of tropical tree species. Science 288: 1414–1418. doi:10.1126/science.288.5470.1414.
- Dorji Y, Schuldt B, Neudam L, Dorji R, Middleby K, Isasa E, Körber K, Ammer C, Annighöfer P & Seidel D (2021) Three-dimensional quantification of tree architecture from mobile laser scanning and geometry analysis. Trees 35: 1385–1398. doi:10.1007/s00468-021-02124-9.
- Engone Obiang NL, Kenfack D, Picard N, Lutz JA, Bissiengou P, Memiaghe HR & Alonso A (2019) Determinants of spatial patterns of canopy tree species in a tropical evergreen forest in Gabon. Journal of Vegetation Science 30: 929–939. doi:10.1111/jvs.12778.
- Erfanifard Y, Nguyen HH, Schmidt JP & Rayburn A (2018) Fine-scale intraspecific interactions and environmental heterogeneity drive the spatial structure in old-growth stands of a dioecious plant. Forest Ecology and Management 425: 92–99. doi:10.1016/j.foreco.2018.05.041.
- Getzin S, Dean C, He F, Trofymow JA, Wiegand K & Wiegand T (2006) Spatial patterns and competition of tree species in a Douglas-fir chronose-quence on Vancouver Island. Ecography 29: 671–682. doi:10.1111/j.2006.0906-7590.04675.x.
- Getzin S, Wiegand T, Wiegand K & He F (2008) Heterogeneity influences spatial patterns and demographics in forest stands. Journal of Ecology 96: 807–820. doi:10.1111/j.1365-2745.2008.01377.x.

- Getzin S, Worbes M, Wiegand T & Wiegand K (2010) Size dominance regulates tree spacing more than competition within height classes in tropical Cameroon. Journal of Tropical Ecology 27: 93–102. doi:10.1017/S0266467410000453.
- Ghalandarayeshi S, Nord-Larsen T, Johannsen VK & Larsen JB (2017) Spatial patterns of tree species in Suserup Skov a semi-natural forest in Denmark. Forest Ecology and Management 406: 391–401. doi:10.1016/j.foreco.2017.10.020.
- Graz FP (2004) The behaviour of the species mingling index $M_{\rm sp}$ in relation to species dominance and dispersion. European Journal of Forest Research 123: 87–92. doi:10.1007/s10342-004-0016-8.
- Hui G, Wang Y, Zhang G, Zhao Z, Bai C & Liu W (2018) A novel approach for assessing the neighborhood competition in two different aged forests. Forest Ecology and Management 422: 49–58. doi:10.1016/j.foreco.2018.03.045.
- Hui G, Zhang G, Zhao Z & Yang A (2019) Methods of forest structure research: a review. Current Forestry Reports 5: 142–154. doi:10.1007/s40725-019-00090-7.
- Kint V, Meirvenne MV, Nachtergale L, Geudens G & Lust N (2003) Spatial methods for quantifying forest stand structure development: a comparison between nearest-neighbor indices and variogram analysis. Forest Science 49: 36–49. doi:10.1093/forestscience/49.1.36.
- Li L, Wei S, Huang Z, Ye W & Cao H (2008) Spatial patterns and interspecific associations of three canopy species at different life stages in a subtropical forest, China. Journal of Integrative Plant Biology 50: 1140–1150. doi:10.1111/j.1744-7909.2008.00690.x.
- Li Y, He J, Yu S, Wang H & Ye S (2020) Spatial structures of different-sized tree species in a secondary forest in the early succession stage. European Journal of Forest Research 139: 709–719. doi:10.1007/s10342-020-01280-w.
- Li Y, He J, Yu S, Zhu D, Wang H & Ye S (2019) Spatial structure of the vertical layers in a subtropical secondary forest 57 years after clear-cutting. iForest 12: 442–450. doi:10.3832/ifor2975-012.
- Li Y, Luo X & Li J (2022) Habitat heterogeneity in karst environments influences the proportion and distribution of random framework. Ecological Indicators 143: 109387. doi:10.1016/j.ecolind.2022.109387.
- Li Y, Ye S, Luo Y, Yu S & Zhang G (2023) Relationship between species diversity and tree size in natural forests around the Tropic of Cancer. Journal of Forestry Research 34: 1735–1745. doi:10.1007/s11676-023-01616-3.
- Lv T, Zhao R, Wang N, Xie L, Feng Y, Li Y, Ding H & Fang Y (2023) Spatial distributions of intra-community tree species under topographically varia-

- ble conditions. Journal of Mountain Science 20: 391–402. doi:10.1007/s11629-022-7642-9.
- Martens SN, Breshears DD & Meyer CW (2000) Spatial distributions of understory light along the grassland/forest continuum: effects of cover, height, and spatial pattern of tree canopies. Ecological Modelling 126: 79–93.
- McIntire EJB & Fajardo A (2009) Beyond description: the active and effective way to infer processes from spatial patterns. Ecology 90: 46–56. doi:10.1890/07-2096.1.
- Muvengwi J, Mbiba M, Chikumbindi J, Ndagurwa HGT & Mureva A (2018) Population structure and spatial point-pattern analysis of a mono stand of *Acacia polyacantha* along a catena in a savanna ecosystem. Forest Ecology and Management 409: 499–508. doi:10.1016/j.foreco.2017.11.056.
- Nguyen HH, Uria-Diez J & Wiegand K (2016) Spatial distribution and association patterns in a tropical evergreen broad-leaved of north-central Vietnam. Journal of Vegetation Science 27: 318–327. doi:10.1111/jvs.12361.
- Paine CE, Norden N, Chave J, Forget PM, Fortunel C, Dexter KG & Baraloto C (2012) Phylogenetic density dependence and environmental filtering predict seedling mortality in a tropical forest. Ecology Letters 15: 34–41. doi:10.1111/j.1461-0248.2011.01705.x.
- Petritan AM, Biris IA, Merce O, Turcu DO & Petritan IC (2012) Structure and diversity of a natural temperate sessile oak (*Quercus petraea* L.) European Beech (*Fagus sylvatica* L.) forest. Forest Ecology and Management 280: 140–149. doi:10.1016/j. foreco.2012.06.007.
- Pinzon J, Wu L, He F & Spence JR (2018) Fine-scale forest variability and biodiversity in the boreal mixedwood forest. Ecography 41: 753–769. doi:10.1111/ecog.03379.
- Pommerening A, Wang H & Zhao Z (2020) Global woodland structure from local interactions: new nearest-neighbour functions for understanding the ontogenesis of global forest structure. Forest Ecosystems 7: 152–162. doi:10.1186/s40663-020-00224-5.
- Potvin C & Dutilleul P (2009) Neighborhood effects and size-asymmetric competition in a tree plantation varying in diversity. Ecology 90: 321–327. doi:10.1890/08-0353.1.
- Remadevi OK, Manjunatha M, Sharma B, Saritha B, Poorvashree P, Suresh HS, Kumar KHV, Kakkar R, Singh RK & Gadow KV (2023) Analysing highly biodiverse tropical dry forests for improved conservation. European Journal of Forest Research 142: 641–656. doi:10.1007/s10342-023-01547-y.
- Schneider EE, Affleck DLR & Larson AJ (2019) Tree spatial patterns modulate peak snow accumulation and snow disappearance. Forest Ecology

- and Management 441: 9-19. doi:10.1016/j.fore-co.2019.03.031.
- Shen G, He F, Waagepetersen R, Sun IF, Hao Z, Chen ZS & Yu M (2013) Quantifying effects of habitat heterogeneity and other clustering processes on spatial distributions of tree species. Ecology 94: 2436–2443. doi:10.1890/12-1983.1.
- Spies TA (1998) Forest structure: a key to the ecosystem. Northwest Science 72: 34–39.
- Wang H, Peng H, Hui G, Hu Y & Zhao Z (2018) Large trees are surrounded by more heterospecific neighboring trees in Korean pine broad-leaved natural forests. Scientific Reporpts 8: 9149. doi:10.1038/s41598-018-27140-7.
- Wang H, Zhang G, Hui G, Li Y, Hu Y & Zhao Z (2016) The influence of sampling unit size and spatial arrangement patterns on neighborhood-based spatial structure analyses of forest stands. Forest Systems 25: e056. doi:10.5424/fs/2016251-07968.
- Wehenkel C, Brazao-Protazio JM, Carrillo-Parra A, Martinez-Guerrero JH, Crecente-Campo F (2015) Spatial distribution patterns in the very rare and species-rich *Picea chihuahuana* tree community (Mexico). PLoS One 10: e0140442. doi:10.1371/journal.pone.0140442.
- Xu H, Hui G, Hu Y, Li C, Lin T, Zhang X & Wu X (2006) Analysis of spatial distribution characteristics of trees with different diameter classes in natural Korean pine broad leaved forest. Forest Research (in Chinese) 19: 687–691.
- Zhang G & Hui G (2021) Random trees are the cornerstones of natural forests. Forests 12: 1046. doi:10.3390/f12081046.
- Zhang G, Hui G, Yang A & Zhao Z (2021) A simple and effective approach to quantitatively characterize structural complexity. Scientific Reports 11: 1326. doi:10.1038/s41598-020-79334-7.
- Zhang G, Hui G, Zhang G, Zhao Z & Hu Y (2019) Telescope method for characterizing the spatial structure of a pine-oak mixed forest in the Xiaolong Mountains, China. Scandinavian Journal of Forest Research 34: 751–762. doi:10.1080/028 27581.2019.1680729.
- Zhang G, Hui G, Zhao Z, Hu Y, Wang H, Liu W & Zang R (2018) Composition of basal area in natural forests based on the uniform angle index. Ecological Informatics 45: 1–8.
- Zhao Z, Hui G, Hu Y, Wang H, Zhang G & Gadow Kv (2014) Testing the significance of different tree spatial distribution patterns based on the uniform angle index. Canadian Journal of Forest Research 44: 1419–1425. doi:10.1139/cjfr-2014-0192.
- Zhu Y, Comita LS, Hubbell SP, Ma K & Shefferson R (2015) Conspecific and phylogenetic density-dependent survival differs across life stages in a tropical forest. Journal of Ecology 103: 957–966. doi:10.1111/1365-2745.12414.